Lawrence Berkeley National Laboratory

Title
Dependence of Gas-Phase Crotonaldehyde Hydrogenation Selectivity and Activity on the Size of Pt Nanoparticles (1.7-7.1 nm) Supported on SBA-15

Permalink
https://escholarship.org/uc/item/71q6g5jc

Author
Grass, Michael

Publication Date
2009-01-15

Peer reviewed

Dependence of gas-phase crotonaldehyde hydrogenation selectivity and activity on the size of Pt nanoparticles (1.7 – 7.1 nm) supported on SBA-15

Michael E. Grass[†], Robert M. Rioux[‡], Gabor A. Somorjai*

Lawrence Berkeley National Laboratory and Department of Chemistry, University of California, Berkeley, California 94720

[†]Current Address: Advanced Light Source, Lawrence Berkeley National Laboratory, Berkeley, CA 94720
[‡]Current address: Department of Chemical Engineering, Pennsylvania State University, University Park, PA 16802-4400

*To whom correspondence should be addressed: somorjai@berkeley.edu

Running title: Influence of particle size on selectivity during crotonaldehyde hydrogenation

Abstract

The selectivity and activity for the hydrogenation of crotonaldehyde to crotyl alcohol and butyraldehyde was studied over a series of Pt nanoparticles (diameter of 1.7, 2.9, 3.6, and 7.1 nm). The nanoparticles were synthesized by the reduction of chloroplatinic acid by alcohol in the presence of poly(vinylpyrrolidone) (PVP), followed by encapsulation into mesoporous SBA-15 silica. The rate of crotonaldehyde hydrogenation and selectivity towards crotyl alcohol both increase with increasing particle size. , The selectivity towards crotyl alcohol increased from 13.7 % to 33.9 % (8 Torr crotonaldehyde, 160 Torr H_2 and 353 K), while the turnover frequency increases from 2.1 $\times$ 10^{-2} s^{-1} to 4.8×10^{-2} s^{-1} with an increase in the particle size from 1.7 nm to 7.1 nm. The decarbonylation pathway to form propene and CO is enhanced over the higher proportion of coordinatively unsaturated sites on the smaller nanoparticles. The apparent activation energy remains constant (~ 16 kcal mol^{-1} for the formation of butyraldehyde and ~ 8 kcal mol^{-1} for the formation of crotyl alcohol) as a function of particle size. In the presence of 130 – 260 mTorr CO, the reaction rate decreases for all products with a CO reaction order of -0.9 for crotyl alcohol and butyraldehyde over 7.1 nm Pt particles; over 1.7 nm Pt particles, the order in CO is -1.4 and -0.9, respectively. Hydrogen reduction at 673 K after calcination in oxygen results in increased activity and selectivity relative to reduction at either higher or lower temperature; this is discussed with regards to the incomplete removal and/or change in morphology of the polymeric surface stabilizing agent, poly(vinylpyrrolidone) used for the synthesis of the Pt nanoparticles..

1. Introduction

Polymer and surfactant stabilized transition metal nanoparticles (NPs) have been utilized as both homogeneous and heterogeneous catalysts over the past decade [1]. Their catalytic ability has been studied extensively both as colloidal suspensions [2] and as oxide- or carbon-supported NPs [3, 4]. The polymer mediated method of metal colloid synthesis can yield transition metal NPs with narrow particle size distribution and has the potential to serve as model systems for the elucidation of particle size effects in heterogeneous catalysis [5, 6].

In our previous work, we developed two strategies for supporting poly(vinylpyrrolidone) (PVP)-protected Pt nanoparticles on mesoporous SBA-15 silica and studied the particle size dependence of the single product reactions (ethylene hydrogenation and ethane hydrogenolysis) and the influence of particle size on the poisoning of ethylene hydrogenation by carbon monoxide [5-9]. In this paper, we report on the selective hydrogenation of crotonaldehyde to crotyl alcohol and butyraldehyde over a series of Pt(X)/SBA-15 (X = 1.7, 2.9, 3.6, and 7.1 nm) catalysts prepared by nanoparticle encapsulation (NE) [5]. We examined the effect of particle size on both the overall conversion of crotonaldehyde and the selectivity towards the industrially desired unsaturated alcohol, crotyl alcohol. We demonstrate NE-synthesized catalysts have similar catalytic activity and selectivity for crotonaldehyde hydrogenation as conventionally-prepared (incipient wetness, ion-exchange, etc.) catalysts [10].

The hydrogenation of crotonaldehyde and other α,β-unsaturated aldehydes is of fundamental scientific interest because of the two distinct unsaturated chemical bonds (C=C and C=O) are present in the same molecule, serving as a useful probe molecule for

studies of heterogeneous catalytic chemoselectivity (**Scheme 1**). Gallezot and Richard summarized many of the properties that determine catalytic activity and selectivity for the conversion of α,β-unsaturated aldehydes by heterogeneous catalysts [10]. Properties of the catalyst that influence both activity and selectivity include the type of metal, the exposed crystal faces of the extended single-crystal or nanoparticle surface, adsorbed ligands (e.g. organometallic tin) and promoters (e.g. K, Fe, Sn) which modify (electronically or geometrically) the surface of the metallic nanoparticle. The structure of the α,β-unsaturated aldehyde influences reaction selectivity. Bulky side groups such as the phenyl group adjacent to the aliphatic double bond in cinnamaldehyde or the pair of methyl groups adjacent to the aliphatic double bond in 3-methyl-crotonaldehyde lead to higher selectivity to the unsaturated alcohol because of steric hindrance of the C=C double bond. In the case of crotonaldehyde, the C=C double bond is flanked by a methyl group only, and the selective hydrogenation of the carbonyl group over the C=C double bond becomes significantly more challenging [10].

In previous investigations of the influence of particle size on the overall turnover frequency (TOF) and selectivity for crotyl alcohol from crotonaldehyde, it was observed that both generally increase with increasing particle size [11-13]. The role of particle size appears to be three-fold. The first is related to the fraction of surface atoms in close packed (111) planes versus atoms at lower coordination sites. Crotonaldehyde adsorbs preferentially via a di-σ bond between the C=O and the Pt(111) surface, while on the (100) surface, it bonds to the surface in a flat η^4 configuration through both of its π-bonds [14]. On the (110) surface, the most corrugated of the three lowest energy fcc surfaces, crotonaldehyde bonds via the C=C π-bond [14]. The increase in selective C=O

interaction on (111) facets is responsible for the increased selectivity towards the unsaturated alcohol. Larger nanoparticles have a larger fraction of surface atoms in terraces with a close-packed structure than do smaller particles and therefore tend to be more selective for the formation of crotyl alcohol [13]. The second particle size effect is the steric hindrance of the C=C bond, which is more easily accommodated on smaller NPs, thus decreasing selectivity towards the unsaturated alcohol over such catalysts. The third effect is decreased catalytic activity over smaller NPs due to decarbonylation of crotonaldehyde to CO and C_3 hydrocarbons as well as other C-C bond breaking reactions occur preferentially on the corner and edge sites that are more prevalent on smaller particles. Adsorbed CO (from decarbonylation) and the carbon fragments deposited due to C-C bond breaking poison the catalyst surface [15].

For the investigation of gas-phase heterogeneous catalysis using polymer encapsulated NPs on oxide supports, the organic capping molecules are typically removed by thermal treatment (pyrolysis, combined calcination and reduction) [6, 16, 17]. In this investigation, we consider the effects of such thermal treatments on the final state of the surface protecting polymer (PVP) and its implication on catalysis.

2. Experimental

2.1 Catalyst Synthesis

The preparation of the Pt nanoparticles (NPs) used in this study and their anchoring in mesoporous SBA-15 silica by nanoparticle encapsulation (NE) has been reported previously [5, 6]. In this study, a series of Pt(X)/SBA-15 ($X = 1.7 - 7.1$ nm) were synthesized with nominal loadings of $1 - 3\%$. Higher weight loading of Pt was used for the catalysts containing larger NPs to account for the decrease in the total surface area of

larger NPs compared to catalysts containing smaller nanoparticles at comparable weight loading. The 1.7 and 7.1 nm NPs were synthesized by the polyol reduction process in ethylene glycol (EG) [6, 18, 19], while 2.9 and 3.6 nm particles were synthesized in an 80/20 v/v mixture of methanol and water by alcohol reduction [6, 20]. The 3.6 nm particles were synthesized by a seeded growth method using the as-synthesized PVP-protected 2.9 nm particles as the seeds [20]. All of the NPs except for the 1.7 nm particles were synthesized in the presence of PVP, which sterically protects the particles from aggregation [21]. The 1.7 nm particles are stabilized electrostatically in a NaOH solution in EG during synthesis, then precipitated from the EG solution and transferred to a volume of ethanol containing PVP.

The nanoparticles were incorporated into silica by synthesizing the mesoporous SBA-15-like silica matrix in neutral pH under hydrothermal conditions in the presence of the PVP-protected NPs [5]. The catalysts were washed in ethanol, dried in air at 373 K and calcined *ex-situ* in O2 at 723 K for 12 h (Pt(2.9 nm)/SBA-15 and Pt(3.6 nm)/SBA-15), at 623 K for 12 h (Pt(1.7 nm)/SBA-15), or at 723 K for 24 h (Pt(7.1 nm)/SBA-15) [6]. After calcination, the catalysts were characterized by X-ray diffraction (XRD) with a Bruker D8 GADDS diffractometer with Co K_α radiation ($\lambda = 1.79$ Å) and transmission electron microscopy (TEM, Philips/FEI Tecnai 12 microscope, 100 kV operating voltage) for confirmation of the bulk particle size. The total surface area and metallic surface area were measured by N_2 physisorption (BET method) and total H_2 chemisorption with a Quantachrome Autosorb 1 automated sorption analyzer. The catalysts were reduced *in-situ* prior to chemisorption by the same protocol used for the reduction of catalysts in reaction studies described below (673 K in H_2 for 2 h) followed by evacuation at 623 K

for 1 h. The catalyst was then cooled to 303 K under vacuum followed by volumetric H_2 chemisorption. The total metal content was determined by inductively coupled plasma – optical emission spectroscopy (ICP-OES) at Galbraith Laboratories (Knoxville, TN USA).

2.2 Catalytic Studies

Catalytic reactions were carried out in a stainless steel (⅛") flow reactor system equipped with mass flow controllers (MKS Instruments) for He, H_2, and O_2 (UHP, Praxair, used as-received) and an inline Pyrex saturator for the introduction of crotonaldehyde (Sigma-Aldrich, 99.9%, predominately *trans*) into the feed. The catalyst was reduced *in situ* at the desired temperature (typically 673 K) for 2 h in H_2 (160 Torr)/He. After cooling to the reaction temperature, the flow of 160 Torr H_2/He was passed through a saturator containing crotonaldehyde held at 273 K using an ice bath. The inlet conditions prior to contact with the catalyst bed was 8 Torr crotonaldehyde, 160 Torr H_2 and balance He.

The catalyst was placed on top of a quartz frit in a ¼" O. D. Pyrex U-tube reactor. For a typical experiment, ~ 15 mg catalyst was diluted with ~ 50 mg acid-washed and calcined low surface area quartz (Sigma Aldrich) and loaded into the reactor between beds of the same acid-washed and calcined quartz. The effluent stream was analyzed by gas chromatography (HP 5890 Series II) using a flame ionization detector (FID) for analysis of organics and a thermal conductivity detector (TCD) for H_2 detection. The reaction was started at 353 K until a stable activity was measured (i.e. until initial deactivation was complete and a steady-state activity was reached); most catalysts required ~ 2.5 h to reach steady state. The reaction temperature was then changed (and

left for 1.5 h at each temperature) to 373, 393, 383, 373, 363, and finally back to 353 K for a check on the extent of catalyst deactivation. Unless stated otherwise, data reported in this paper is the steady-state rate at 353 K (the deactivation check measurement). The activation energy for all samples was determined using the rates obtained while cooling from 393 to 353 K. The conversion at each temperature was averaged from ten GC injections. The TOF was calculated by normalizing the reaction rate to the number surface Pt atoms based on TEM measurements and the Pt loading determined by ICP-OES. Selectivity values were calculated by dividing the TOF a particular product by the overall TOF (the rate of disappearance of crotonaldehyde).

CO poisoning experiments were conducted at 353 K in the same manner described above, but with the addition of 1% CO in He (Praxair, UHP) corresponding to CO partial pressures of 134 – 262 mTorr in the feed stream.

3. Results and Discussion

3.1 Catalyst Properties

The as-synthesized NPs were analyzed by TEM and XRD before encapsulation and the SBA-15-supported Pt catalysts were characterized by ICP-OES, TEM, XRD, and chemisorption after calcination. An exhaustive analysis of the characteristics of these catalysts has been given previously and no notable deviations from the previous report were observed [5]. The metal loading determined by ICP-OES analysis, the metal dispersion determined from H_2 chemisorption measurements, and a summary of the catalytic results are listed in Table 1. The particle size determined from TEM and XRD line-broadening (determined using the Scherrer equation) are in agreement and analysis

of the TEM images indicates a standard deviation in particle size of ~ 10 % for all catalysts.

The dispersion measured by total hydrogen chemisorption are ~ 50 % lower than the measured TEM results. The theoretical H/Pt_T (total Pt) ratio for 1.7, 2.9, 3.6, and 7.1 nm Pt NPs are 0.66, 0.39, 0.31, and 0.16, respectively, assuming hemispherical particles and 1:1 stoichiometry between H and Pt_s (surface Pt). This discrepancy suggests that the *ex situ* calcination - *in situ* reduction procedure described in the experimental section produce catalysts capable of adsorbing hydrogen up to only 50% coverage relative to the total number of surface Pt atoms, regardless of particle size. The suppressed adsorption of hydrogen is likely due to blockage of surface sites by residual carbonaceous material from the decomposition of PVP during the oxygen and hydrogen pretreatment steps. The fractional coverage of this layer as measured by H_2 chemisorption is independent of particle size. In a study by Du *et al.*, PVP-protected Pt (2.5 nm) nanoparticles were heated in N_2 for 0.5 h at 773 K: after the heat treatment, the molar $C:Pt_s$ ratio was 35 (before thermal treatment, the ratio was 85) [22]. In this work, we have used oxygen pretreatment for a much longer time (12 – 24 h), but it appears that residual carbon from either PVP or P123 remains on the Pt surface. The surface coverage and chemical composition of this layer may play a significant role in the catalytic properties of the calcined/reduced Pt nanoparticles.

3.2 Crotonaldehyde Hydrogenation

Butyraldehyde formed by the selective hydrogenation of the C=C bond in crotonaldehyde, is the major product of crotonaldehyde hydrogenation over all catalysts and the entire temperature range (353 – 393 K) studied. The minor products are crotyl

alcohol (the second most abundant product) formed by selective hydrogenation of the C=O bond, butanol (hydrogenation of both the C=C and C=O bonds), and propylene and propane (decarbonylation) (Scheme 1).

The initial time-on-stream data for Pt(1.7 nm)/SBA-15 and Pt(7.1 nm)/SBA-15 shows an initial deactivation period that lasts ~2.5 h. It is well-documented in the literature that this deactivation is a result of decarbonylation and the subsequent adsorption of CO on the Pt surface, as well as the deposition of carbon resulting from C-C and C-H bond scission [23-26]. C_3 hydrocarbons produced from the decarbonylation pathway were detected at all reaction temperatures and on all catalysts, indicating the formation of CO (although CO was not detected in the gas-phase by gas chromatography). The initial TOF for decarbonylation is at least 10^{-3} s^{-1} for all four catalysts. If we assume that the CO formed by decarbonylation remains on the surface, enough CO forms to saturate the Pt surface sites (based on the number of surface atoms determined by TEM measurements) within 15-20 min after the start of the reaction. The deactivation of heterogeneous catalysts for the hydrogenation of α,β-unsaturated aldehydes by CO as a result of decarbonylation has been revealed in surface science studies [26], infrared spectroscopy studies on supported catalysts [24], and kinetic studies [25] over a number of different transition metals. A second pathway for deactivation is coke formation from C-C bond rupture. This process may be slower than the formation of CO by decarbonylation, but the products of this process will not desorb during reaction.

The temperature dependence for hydrogenation is similar for all catalysts studied. The overall apparent activation energy for the disappearance of crotonaldehyde is independent of the particle size (Table 1). The apparent activation energy for the

individual products is also not dependent on particle size: 16 – 17 kcal mol^{-1} for C=C

hydrogenation to butyraldehyde, 7 – 10 kcal mol^{-1} for C=O hydrogenation to crotyl

alcohol, 10 – 15 kcal mol^{-1} for the complete hydrogenation to butanol, and 11 – 12 kcal

mol^{-1} for decarbonylation. The temperature dependence for all products catalyzed by

Pt(7.1 nm)/SBA-15 is shown in Figure 1. Lower temperatures favor the formation of

minor products (particularly crotyl alcohol) relative to butyraldehyde (the apparent

activation energy for the formation of butyraldehyde is higher than for the formation of

crotyl alcohol over all catalysts studied). Butyraldehyde is the more thermodynamically-

favored product, but it is also the more kinetically-hindered (higher apparent activation

energy). These observations are consistent with general trends of crotonaldehyde

hydrogenation over Pt catalysts that have been reported previously [10].

3.3 Particle Size Effects on Selectivity and Activity for Crotonaldehyde Hydrogenation

The reaction selectivity to crotyl alcohol and steady-state TOF at 353 K for all

catalysts is listed in Table 1 and shown in **Figures 2 and 3**. The overall rate and

selectivity to crotyl alcohol increased linearly with increasing particle size. The steady-

state rate increased by a factor of two (from 2.4×10^{-2} s^{-1} to 4.8×10^{-2} s^{-1}) and the

selectivity towards crotyl alcohol varied by a factor of ~ 3 (from 13.7 % to 33.9 %) with

an increase in the particle size from 1.7 to 7.1 nm. The increase in selectivity toward

crotyl alcohol with particle size results mainly from the increased interaction of C=O

with terrace sites on Pt [10, 14, 27].

The initial deactivation is also dependent on particle size. During the first 10 minutes

on stream, Pt(1.7 nm)/SBA-15 is 1.5 times more active than Pt(7.1 nm)/SBA-15 ($6.9 \times$

10^{-2} s^{-1} versus 4.7×10^{-2} s^{-1} at 353 K). While both catalysts have the same initial TOF for

butyraldehyde production, the Pt(1.7 nm)/SBA-15 is 1.5 times more active for the formation of crotyl alcohol, seven times more active for complete hydrogenation to butanol, and three times more active for decarbonylation at the onset of the reaction (Figure 4). The three-fold higher TOF for decarbonylation explains the larger extent of deactivation over Pt(1.7 nm)/SBA-15 compared to Pt(7.1 nm)/SBA-15. The initial TOF for decarbonylation (based on the appearance of propene and propane) over the four catalysts is 2.5×10^{-3}, 1.8×10^{-3}, 1.0×10^{-3}, and 1.0×10^{-3} s^{-1} for Pt(1.7 nm)/SBA-15 (3.3-fold decrease in activity from initial-to-steady state), Pt(2.9 nm)/SBA-15 (2.3-fold decrease), Pt(3.6 nm)/SBA-15 (1.8-fold decrease), and Pt(7.1 nm)/SBA-15 (1.8-fold decrease), respectively (inset in **Figure 4A**). After the initial period of deactivation, the rate of decarbonylation is the same over the Pt(X)/SBA-15 catalysts. At longer time-on-stream, the decreased activity of Pt(1.7 nm)/SBA-15 results from the formation of coke formation. The increased amount of decarbonylation and coke formation over the smaller 1.7 nm particles likely results from the increased C-C bond scission activity of low-coordination sites that predominate on smaller nanoparticles.

3.4 CO Poisoning

CO poisoning was tested over the series of Pt(X)/SBA-15 catalysts by the addition of small quantities of CO to the feed. Reaction rates were measured over Pt(1.7 nm)/SBA-15 and Pt(7.1 nm)/SBA-15 at 353 K as described above with the addition of a low pressure of CO (134 – 262 mTorr CO). For both catalysts, the overall reaction rate decreased by ~ 70% in the presence of 134 mTorr CO relative to the rate before the addition of CO. The rate of formation of C_3 hydrocarbons and butanol in the presence of CO was detectable, but too low for accurate determination of the TOF. The reaction

order at 353 K in CO on the Pt(1.7 nm)/SBA-15 was – 0.9 and -1.4 for butyraldehyde and crotyl alcohol, respectively, For the Pt(7.1 nm)/SBA-15, the reaction order in CO was -0.9 for both products (**Figure 5**). The negative reaction order in CO suggests it is the most abundant surface intermediate during the hydrogenation of crotonaldehyde in the presence of 130 – 260 mTorr CO [28]. The partial pressure of CO under reaction conditions (in the absence of CO) due to decarbonylation (~ 15 mTorr based on the rate of C_3 production) is much lower than the pressure of CO added through the 1% CO/He mixture. The reaction order for crotyl alcohol formation over Pt(1.7 nm)/SBA-15 is more negative than over Pt(7.1 nm)/SBA-15. While this is not completely understood, it appears to be consistent with the larger decrease in crotyl alcohol formation over Pt(1.7 nm)/SBA-15

3.5 Effect of Reduction Temperature on Catalyst Activity and Selectivity

The effect of the reduction temperature was studied on Pt(*X*)/SBA-15 catalysts. All samples were calcined in O_2 at high temperature in a horizontal tube furnace, followed by reduction in H_2 (as described previously) in the U-tube reactor immediately prior to the hydrogenation of crotonaldehyde. All samples show an optimal reduction temperature of between 673 and 723 K with lower and higher reduction temperatures resulting in a decrease in the overall conversion rate of crotonaldehyde as well as a lower selectivity towards crotyl alcohol (**Figure 6** shows this trend for Pt(7.1 nm)/SBA-15). Particle sintering, which has been observed in many studies of Pt nanoparticles supported on SiO_2 [29], is ruled out as the cause of these changes based on TEM observations of the catalysts before and after high temperature reduction.

Residual carbon from the decomposition of PVP likely remains on the surface of the Pt nanoparticles after calcination and reduction. The amount and chemical state of this carbon will depend on the treatment time and temperature. Borodko *et al.* have shown that the carbonyl group of PVP interacts mores strongly with Pt NPs when oxidized in air at 363 K than when reduced in H_2 at 363 K [30]. Coloma *et al.* studied the effect of reduction temperature for Pt/activated carbon catalysts in the hydrogenation of crotonaldehyde. They found that the type of oxygenated species on the support and the reduction temperature significantly changed the activity and selectivity of the catalyst [31]. The carbonyl groups in PVP may be similarly important for PVP stabilized Pt NP catalysts. The role of stabilizing molecules in catalysis is important and its effect on the catalytic performance of colloidally prepared NPs has not been adequately studied. Even after thermal treatment in O_2 at 623 – 723 K, some organic overlayer remains on the Pt surface and is modified by subsequent H_2 treatment [30].

4. Conclusions

Monodisperse Pt nanoparticles (1.7 – 7.1 nm) synthesized by the reduction of chloroplatinic acid in alcohol containing poly(vinylpyrrolidone) were supported on mesoporous SBA-15 silica by nanoparticle encapsulation for the hydrogenation of crotonaldehyde. Solution phase synthesis of Pt nanoparticles provide excellent control over particle size and size distribution, allowing for better understanding of the effect of particle size on *selectivity* in catalysis. Both the activity and selectivity towards crotyl alcohol increased with increasing particle size. As the particle size increased from 1.7 to 7.1 nm, the turnover frequency increased from 2.1×10^{-2} to 4.8×10^{-2} s^{-1} and the selectivity to crotyl alcohol increases from 14 % to 34 % (353 K and H_2/crotonaldehyde ratio of 20).

The initial rate of decarbonylation is also particle size dependent: the TOF is 2.5×10^{-3} over Pt(1.7 nm)/SBA-15 and 1.0×10^{-3} over Pt(7.1 nm)/SBA-15. The increased rate of decarbonylation over catalysts with smaller Pt particles appears responsible for the increased deactivation. The reduction temperature significantly influenced both the activity and selectivity; there is an optimal reduction temperature of 673 K for 7.1 nm Pt nanoparticle catalysts.

Acknowledgements

References

[1]   J. D. Aiken and R. G. Finke, J. Mol. Catal. A: Chem. 145 (1999) 1.

[2]   A. Roucoux, J. Schulz and H. Patin, Chem. Rev. 102 (2002) 3757.

[3]   H. F. Lang, R. A. May, B. L. Iversen and B. D. Chandler, J. Am. Chem. Soc. 125 (2003) 14832.

[4]   Z. Konya, V. F. Puntes, I. Kiricsi, J. Zhu, J. W. Ager, M. K. Ko, H. Frei, P. Alivisatos and G. A. Somorjai, Chem. Mater. 15 (2003) 1242.

[5]   H. Song, R. M. Rioux, J. D. Hoefelmeyer, R. Komor, K. Niesz, M. Grass, P. D. Yang and G. A. Somorjai, J. Am. Chem. Soc. 128 (2006) 3027.

[6]   R. M. Rioux, H. Song, J. D. Hoefelmeyer, P. Yang and G. A. Somorjai, J. Phys. Chem. B 109 (2005) 2192.

[7]   R. M. Rioux, J. D. Hoefelmeyer, M. Grass, H. Song, K. Niesz, P. D. Yang and G. A. Somorjai, Langmuir 24 (2008) 198.

[8]   R. M. Rioux, R. Komor, H. Song, J. D. Hoefelmeyer, M. Grass, K. Niesz, P. D. Yang and G. A. Somorjai, J. Catal. 254 (2008) 1.

[9]   M. E. Grass, Y. Yue, S. E. Habas, R. M. Rioux, C. I. Teall, P. Yang and G. A. Somorjai, J. Phys. Chem. C 112 (2008) 4797.

[10]   P. Gallezot and D. Richard, Cat. Rev. - Sci. Eng. 40 (1998) 81.

[11]   G. F. Santori, M. L. Casella, G. J. Siri, H. R. Aduriz and O. A. Ferretti, React. Kinet. Catal. Lett. 75 (2002) 225.

[12]   A. Giroir-Fendler, D. Richard and P. Gallezot, Catal. Lett. 5 (1990) 175.

[13]   M. Englisch, A. Jentys and J. A. Lercher, J. Catal. 166 (1997) 25.

[14]   F. Delbecq and P. Sautet, J. Catal. 152 (1995) 217.

[15]   A. B. Merlo, G. F. Santori, J. Sambeth, G. J. Siri, M. L. Casella and O. A. Ferretti, Catal. Commun. 7 (2006) 204.

[16]   A. M. Venezia, L. F. Liotta, G. Pantaleo, V. La Parola, G. Deganello, A. Beck, Z. Koppany, K. Frey, D. Horvath and L. Guczi, Appl. Catal. A: Gen. 251 (2003) 359.

[17]   D. S. Deutsch, A. Siani, P. T. Fanson, H. Hirata, S. Matsumoto, C. T. Williams and M. D. Amiridis, J. Phys. Chem. C 111 (2007) 4246.

[18]   H. Song, F. Kim, S. Connor, G. A. Somorjai and P. D. Yang, J. Phys. Chem. B 109 (2005) 188.

[19]   Y. Wang, J. Ren, K. Deng, L. Gui and Y. Tang, Chem. Mater. 12 (2000) 1622.

[20]   T. Teranishi, M. Hosoe, T. Tanaka and M. Miyake, J. Phys. Chem. B 103 (1999) 3818.

[21]   R. B. Grubbs, Polym. Rev. 47 (2007) 197

[22]   Y. K. Du, P. Yang, Z. G. Mou, N. P. Hua and L. Jiang, J. Appl. Poly. Sci. 99 (2006) 23.

[23]   T. Birchem, C. M. Pradier, Y. Berthier and G. Cordier, J. Catal. 146 (1994) 503.

[24]   A. Waghray and D. G. Blackmond, J. Phys. Chem. 97 (1993) 6002.

[25]   U. K. Singh and M. A. Vannice, J. Catal. 191 (2000) 165.

[26]   R. Shekhar and M. A. Barteau, Surf. Sci. 319 (1994) 298.

[27]   P. Beccat, J. C. Bertolini, Y. Gauthier, J. Massardier and P. Ruiz, J. Catal. 126 (1990) 451.

[28]   M. Boudart, AIChE J. 18 (1972) 465.

[29]   R. T. K. Baker, E. B. Prestridge and R. L. Garten, J. Catal. 56 (1979) 390.

[30]   Y. Borodko, S. M. Humphrey, T. D. Tilley, H. Frei and G. A. Somorjai, J. Phys. Chem. C 111 (2007) 6288.

[31]   F. Coloma, A. Sepulveda-Escribano, J. L. G. Fierro and F. Rodriguez-Reinoso, Appl. Catal. A: Gen. 150 (1997) 165.

Table 1: Physiochemical properties and summary of catalytic results for Pt(X)/SBA-15 catalysts

Catalyst	Pt Loading[a] (% Pt)	TEM Size (nm)	H_{tot}/Pt[b]	TOF $(100 \times s^{-1})$[c]	$S_{crotyl\ alcohol}$[d]	E_a (kcal mol^{-1})[e]
Pt(1.7 nm)/SBA-15	0.58	1.7	0.33	2.4	13.7	10.8
Pt(2.9 nm)/SBA-15	1.28	2.9	0.18	2.6	17.0	11.2
Pt(3.6 nm)/SBA-15	1.61	3.6	0.15	3.6	21.6	10.8
Pt(7.1 nm)/SBA-15	2.43	7.1	0.08	4.8	33.9	11.7

[a] Loading determined by ICP-OES.
[b] Total H_2 chemisorption at 303 K, extrapolated to P = 0.
[c] Overall steady-state crotonaldehyde hydrogenation rate per surface site at 8 Torr C_6H_4O, 160 Torr H_2 and 353 K.
[d] Determined at 8 Torr crotonaldehyde, and 160 Torr H_2 and 353 K.
[e] Overall apparent activation energy determined at 8 Torr crotonaldehyde, 160 Torr H_2, and 353 – 393 K.
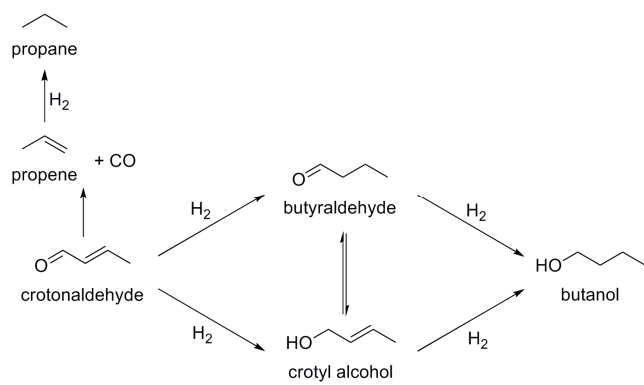
Scheme 1. Reaction network for the conversion of crotonaldehyde in hydrogen.
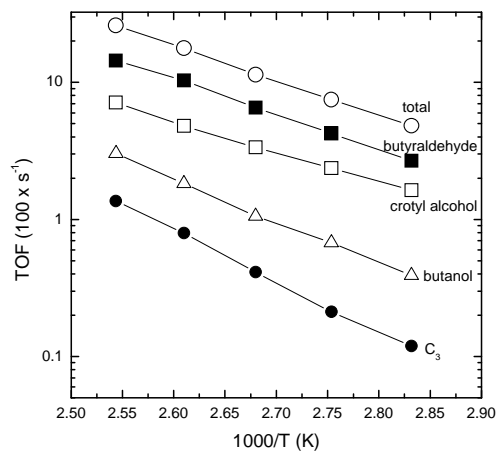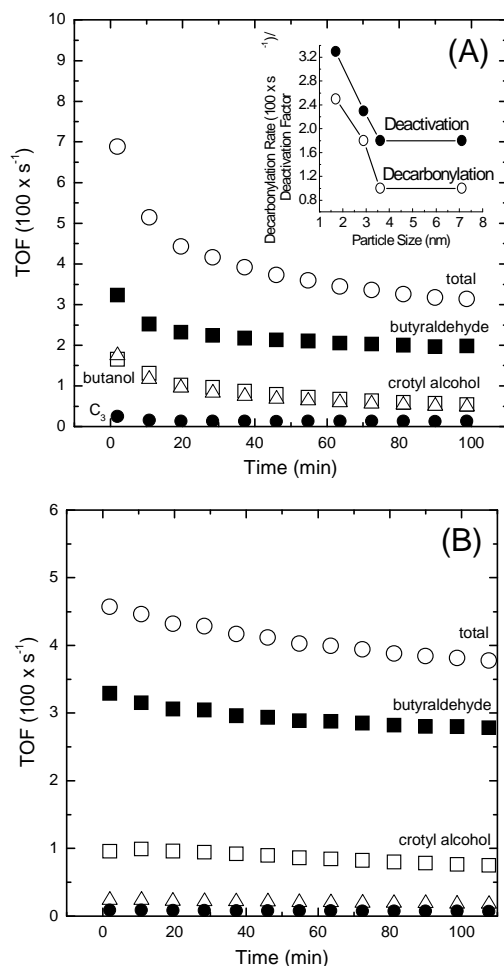
Figure 1. Turnover frequency for the disappearance of crotonaldehyde (○) and formation of butyraldehyde (■), crotyl alcohol (□), butanol (Δ), and C_3 hydrocarbons (●) as an Arrhenius plot for Pt(7.1 nm)/SBA-15. The pressure of crotonaldehyde and hydrogen was 8 Torr and 160 Torr (760 Torr total pressure). The apparent activation energy is 12 kcal mol^{-1} (overall), 17 kcal mol^{-1} (butyraldehyde), 10 kcal mol^{-1} (crotyl alcohol), 14 kcal mol^{-1} (butanol), and 12 kcal mol^{-1} (C_3 hydrocarbons).
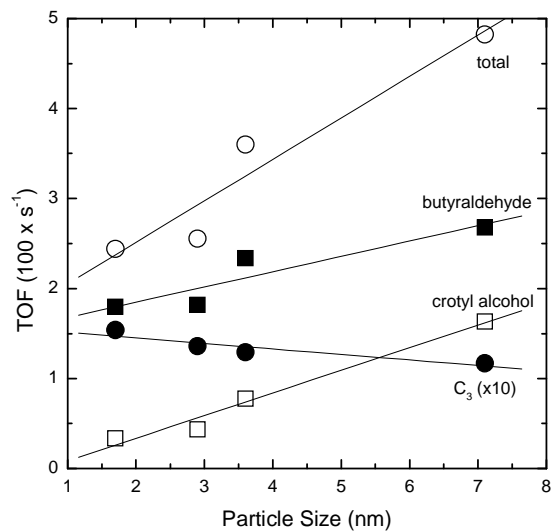
Figure 2: Selectivity as a function of particle size at 353 K for butyraldehyde (■), crotyl alcohol (□), and C_3 hydrocarbons (●). The selectivity towards crotyl alcohol increased with increasing particle size, while the selectivity to butyraldehyde decreased. The pressure of crotonaldehyde and hydrogen was 8 Torr and 160 Torr (760 Torr total pressure).
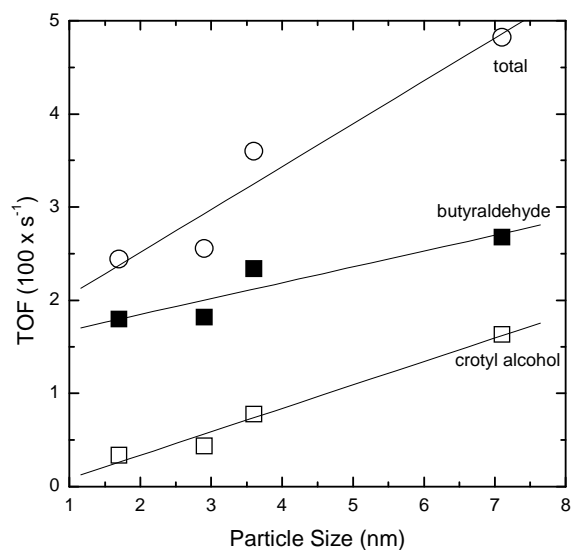
Figure 3: Turnover frequency as a function of particle size at 353 K for butyraldehyde (■) and crotyl alcohol (□). The overall TOF (○) increases with particle size, but more strongly for the formation of crotyl alcohol. The pressure of crotonaldehyde and hydrogen was 8 Torr and 160 Torr (760 Torr total pressure).

Figure 4. Initial deactivation of (A) Pt(1.7 nm)/SBA-15 and (B) Pt(7.1 nm)/SBA-15 with time-on-stream at 353 K. The initial overall turnover frequency is greater for the 1.7 nm particles, but they demonstrate a greater extent of deactivation (presumably due to the greater rate of decarbonylation). The disappearance of crotonaldehyde (○) and the formation of butyraldehyde (■), crotyl alcohol (□), butanol (Δ), and C_3 hydrocarbons (●) are shown. The inset shows the initial rate of decarbonylation (○) and the amount of deactivation (●), where the deactivation factor is expressed as initial rate/steady state rate for the disappearance of crotonaldehyde. The pressure of crotonaldehyde and hydrogen was 8 Torr and 160 Torr (760 Torr total pressure).
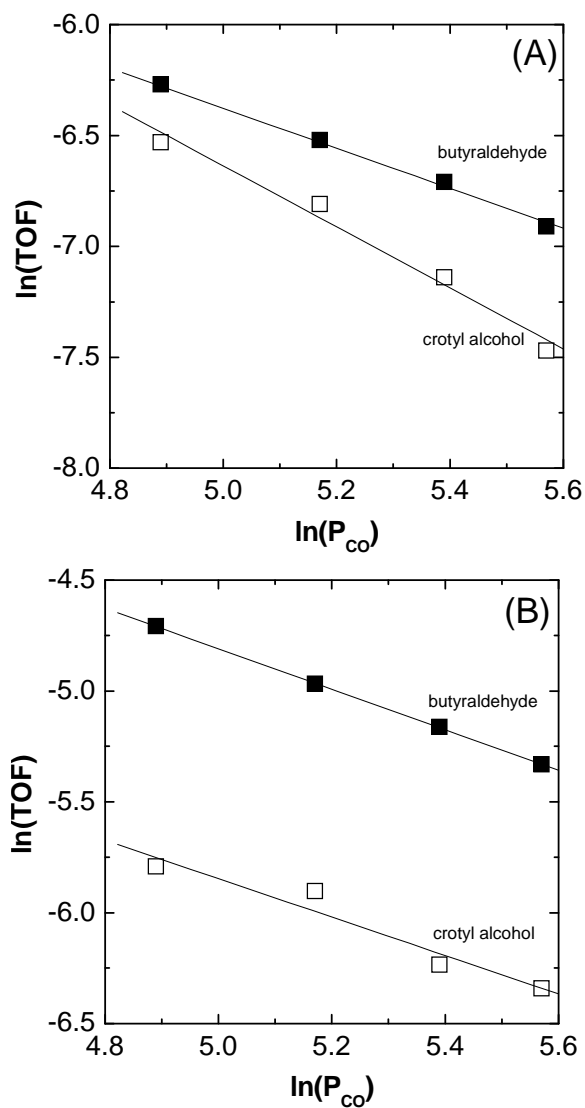
Figure 5. The dependence of the rate of butyraldehyde (■) and crotyl alcohol (□) formation on the pressure of CO for (A) Pt(1.7 nm)/SBA-15 and (B) Pt(7.1 nm)/SBA-15. The reaction conditions were 353 K, 8 Torr crotonaldehyde, 160 Torr H_2, 134 – 262 mTorr CO in a balance He.
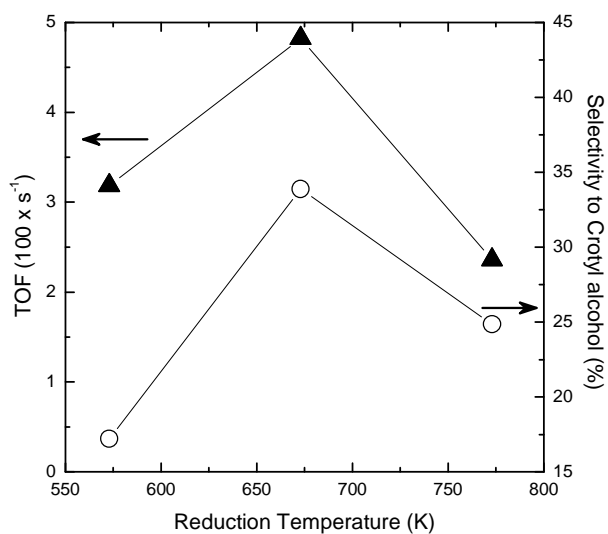
Figure 6. Overall turnover frequency (▲) and selectivity (○) to crotyl alcohol at 353 K over Pt(7.1 nm)/SBA-15 as a function of the reduction temperature (after calcination at 723 K for 24 h). The overall TOF is maximized after reduction at 673 K. The pressure of crotonaldehyde and hydrogen was 8 Torr and 160 Torr (760 Torr total pressure).